

## Rational Magnetic Modification of N,N-Dioxide Pyrazine Ring Expanded Adenine and Thymine: Diradical Character Induced by Base Pairing and Double Protonation

Dongxiao Chen, Yuxiang Bu\*

*School of Chemistry and Chemical Engineering, Shandong University, Jinan, 250100, People's Republic of China*

### Electronic Supplementary Information

**Table S1** The calculated energies (in a.u.) of close-shell singlet (CS) state and triplet (T) state for noA, noT and all the one-step modified intermediate configurations.

Base pairs	$E_{(CS)}/a.u.$	$E_{(T)}/a.u. (\langle S^2 \rangle)$
noT	-790.4065136	-790.3562421 (2.013)
noA	-803.5732712	-803.5335132 (2.012)
noT-A	-1257.8790621	-1257.8289672 (2.013)
noA-T	-1257.8681876	-1257.8275983 (2.012)
nohT	-790.9459260	-790.8689919 (2.012)
noh45A	-804.1431235	-804.0912637 (2.024)
noh74A	-804.1558169	-804.0942573 (2.021)
noh75A	-804.1218558	-804.0853640 (2.017)
noh37A	-804.1677125	-804.1314158 (2.012)
noh34A	-804.1547827	-804.0935766 (2.013)
noh35A	-804.1614564	-804.1037404 (2.009)

† The corresponding author: Yuxiang Bu, e-mail: byx@sdu.edu.cn

**Table S2** Single point calculations for energies (in a.u.) and  $\langle S^2 \rangle$  values of broken-symmetry open-shell singlet (BS) state and magnetic exchange coupling constants  $J$  (in  $\text{cm}^{-1}$ ) of all the modified base pairs at the B3LYP/6-311++G(3df,3pd) and B3LYP/aug-cc-PVTZ levels based on the B3LYP/6-311++g(d,p) geometries.

Base pairs	B3LYP/6-311++G(3df,3pd)		B3LYP/aug-cc-PVTZ	
	$E_{\text{(BS)}}/\text{a.u.} (\langle S^2 \rangle)$	$J/\text{cm}^{-1}$	$E_{\text{(BS)}}/\text{a.u.} (\langle S^2 \rangle)$	$J/\text{cm}^{-1}$
<b>nohT-A</b>	-1258.5735759 (0.860)	-237.9	-1258.5982311 (0.859)	-235.3
<b>noh45A-T</b>	-1258.5676954 (0.356)	-2350.9	-1258.592678 (0.355)	-2367.2
<b>noh74A-T</b>	-1258.5744872 (0.209)	-3017.4	-1258.5995014 (0.208)	-3025.5
<b>noh75A-T</b>	-1258.5414945 (0.395)	-1479.5	-1258.5659797 (0.394)	-1475.5
<b>noh37A-T</b>	-1258.5867487 (0.000)	—	-1258.6118282 (0.000)	—
<b>noh34A-T</b>	-1258.5757472 (0.000)	—	-1258.6003225 (0.000)	—
<b>noh35A-T</b>	-1258.5912404 (0.000)	—	-1258.6162895 (0.000)	—

**Table S3** The calculated  $J$  values of seven topic base pairs by using different functionals including B3LYP, PBE0, wB97XD and M06-2X with 6-311++g(d,p) basis set for optimization. DM denotes diamagnetic, and “-” denotes the corresponding B3LYP geometry is not observed.

Base pairs	B3LYP	PBE0	wB97XD	M06-2X
<b>nohT-A</b>	-194.6	-67.7	-	-
<b>noh45A-T</b>	-2147.2	-1753.7	DM	-
<b>noh74A-T</b>	-2807.4	DM	DM	-
<b>noh75A-T</b>	-1279.7	-900.0	DM	-
<b>noh37A-T</b>	DM	DM	DM	-
<b>noh34A-T</b>	DM	DM	DM	-
<b>noh35A-T</b>	DM	DM	DM	DM

**Note: The test of different functionals.** As shown in Table S3, the calculated magnetic properties of seven topic base pairs are varied when using different functionals for optimizations and energy calculations. In general, PBE0 functional provides the closest results with B3LYP, but it underestimates the magnetic coupling interaction (except for estimated DM noh74A-T), reflecting in the lower  $|J|$  values than B3LYP results. M06-2X and

wB97XD both have totally different results with B3LYP, and both cannot get the proper geometry of nohT-A. In the case of six nohA-Ts, wB97XD overestimates the magnetic coupling interaction, because it gives the right geometries but DM results, while M06-2X only gives six corresponding DM single proton transfer products mentioned in section 3.4 (b). Therefore, it is crucial to choose the best functional for discussion. Given that B3LYP has a good performance in similar systems and can yield quite consistent results with the CASSCF method, it is finally chosen to be the main theoretical method in this work.

**Table S4** The CASSCF(10,10)/6-311++G(d,p)-estimated occupation numbers (occ. n.) of LUNO and energy difference (absolute value) between the BS and T states ( $\Delta E_{BS-T}$ , kcal/mol), compared with  $\langle S^2 \rangle$  values of the BS states and  $\Delta E_{BS-T}$  estimated by the unrestricted B3LYP/6-311++G(d,p) method for all seven topic molecules.

Base pairs	CASSCF(10,10) /6-311++G(d,p)		B3LYP/6-311++G(d,p)	
	LUNO(occ. n.)	$\Delta E_{BS-T}$	$\langle S^2 \rangle_{BS}$	$\Delta E_{BS-T}$
<b>nohT-A</b>	0.995	0.81	0.864	0.64
<b>noh45A-T</b>	0.115	9.36	0.373	10.11
<b>noh74A-T</b>	0.129	20.25	0.226	14.44
<b>noh75A-T</b>	0.192	3.10	0.412	5.89
<b>noh37A-T</b>	0.000	50.87	0.000	19.60
<b>noh34A-T</b>	0.000	30.57	0.000	24.29
<b>noh35A-T</b>	0.000	34.03	0.000	26.74

**Table S5** The calculated HOMO-LUMO gaps (in eV) of six nohA-Ts at the B3LYP/6-311++G(d,p) and MP2/6-311++G(d,p) levels based on the former geometries

Base pairs	B3LYP	MP2
<b>noh45A-T</b>	0.431	4.753
<b>noh74A-T</b>	0.463	5.546
<b>noh75A-T</b>	0.395	4.979
<b>noh37A-T</b>	0.709	6.298
<b>noh34A-T</b>	0.877	6.872
<b>noh35A-T</b>	2.197	7.928

**Table S6** The protonation energies (kcal/mol) of all possible protonation processes for generating the topic base pairs. **Note:** **i)** The data on diagonal (in bold) represent the first protonation energy, e.g. 239.89 in row “3” and column “3” means the protonation energy of nohA-T becoming noh3A-T is 239.89 kcal/mol; **ii)** all off-diagonal data are the second protonation energies. The number at the cross of row (M) and column (N) denotes the protonation energy of the protonated nohMA-T becoming diprotonated nohMNA-T, e.g. 142.70 at the cross of row “4” and column “3” means the protonation energy of noh4A-T (becoming noh34A-T) is 142.70 kcal/mol; **iii)** the protonation site “1” and “2” in nohT-A mean the protonation site which is close to and far from the methyl group, respectively.

nohA-T	3	4	5	7	nohT-A	1	2
3	<b>239.89</b>	140.94	150.55	148.02	1	<b>242.80</b>	130.70
4	142.70	<b>238.13</b>	138.25	142.52	2	147.40	<b>226.10</b>
5	164.27	150.22	<b>226.17</b>	134.09			
7	167.55	160.29	139.90	<b>220.36</b>			

**Table S7** The calculated energies (in a.u.) of the ground states of all seven two-steps modified base pairs when using H<sub>3</sub>O<sup>+</sup> auxiliary group for double protonation, and *J* values for AFM base pairs and the energy difference of the CS and T state for DM base pairs at the B3LYP/6-311++g(d,p) method. “origin” in the table denotes the relevant data of corresponding topic base pairs, for example, “*J* (origin)” of “noh3oT-A” row denotes the *J* value of nohT-A.

Base pairs (AFM)	E <sub>(BS)</sub> /a.u. (<S <sup>2</sup> >)	<i>J</i> /cm <sup>-1</sup>	<i>J</i> (origin)
noh3oT-A	-1411.443798 (0.592)	-738.7	-194.6
noh3o75A-T	-1411.431025 (0.040)	-2825.0	-1279.7
Base pairs (DM)	E <sub>(CS)</sub> /a.u.	ΔE <sub>CS-T</sub> /kcal·mol <sup>-1</sup>	ΔE <sub>CS-T</sub> (origin)
noh3o74A-T	-1411.4586263	22.60	13.97
noh3o45A-T	-1411.4509946	17.67	8.70
noh3o37A-T	-1411.4687005	31.92	19.60
noh3o34A-T	-1411.4625039	23.38	24.29
noh3o35A-T	-1411.4673018	27.82	26.74

**Table S8** B3LYP estimated binding energies (B.E.) of modified base and pairing base in seven topic base pairs (-12.66 kcal/mol for a normal A-T base pair), which is calculated as B.E. = E(base pair) – E(modified base) – E(pairing base). Calculated the magnetic properties and energies of the ground state of the possible single proton transfer products of topic base pairs.

Base pairs	B.E. /kcal·mol <sup>-1</sup>	1h-isomers	Magnetism	E <sub>(ground)</sub> /a.u.
<b>nohT-A</b>	-48.21	<b>nohT-A(h)</b>		unobserved
<b>noh45A-T</b>	-30.83	<b>noh45A-T(h)</b>	DM	-1258.4690958
<b>noh74A-T</b>	-27.13	<b>noh74A-T(h)</b>	DM	-1258.4761033
<b>noh75A-T</b>	-28.05	<b>noh75A-T(h)</b>	AFM(-2127.7 cm <sup>-1</sup> )	-1258.4382184
<b>noh37A-T</b>	-26.92	<b>noh37A-T(h)</b>	DM	-1258.4905309
<b>noh34A-T</b>	-27.96	<b>noh34A-T(h)</b>	DM	-1258.4806670
<b>noh35A-T</b>	-33.38	-		

**Note:** BSSE (Basis Set Superposition Error) method is not used in B.E. calculations because of the following two reasons: (i) Calculated B.E. values are not too small, which also confirms the polarized H-bond that is similar to a chemical bond, so BSSE method may not suitable for improving accuracy. (ii) The charge and spin multiplicity of modified base and pairing base are hard to define, since the diradical character is induced by charge transfer and electron separation between two bases.

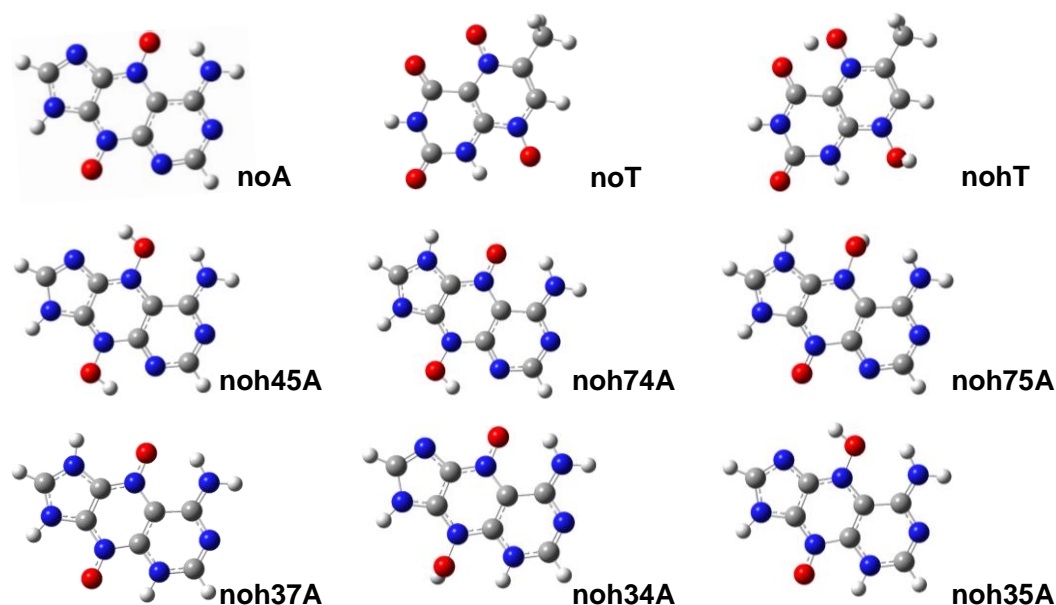


**Fig. S1** The optimized geometries of noT, noA, nohT and all the possible nohA configurations.

**The reasons of DM character in noA and noT.** Since in two precursors, noA and noT, two nitroxide groups can be seen as two radicals and are located on the para-position of the expanded ring, an open-shell singlet state should be stable at the first glance. However, as shown in Table S1, the CS ground states show they both have an excessive spin coupling and DM characters, which is mainly due to the special coupling mode in such a para-position N,N-dioxide system. Our recent work (D. X. Chen, T. G. Deng, L. Yang and Y. X. Bu, *J. Phys. Chem. C*, 2019, **123**, 14152-14163) has investigated the spin coupling properties based on the experimentally synthesized phenazine-N,N'-dioxide (PDO) before, and found that the bond type of the coupling path and the chemical environment around the nitroxide group are two critical factors to influence the coupling mode in such a system. In the noT case, Fig. S1 clearly show that two nitroxide groups are closely link to two C=C bonds, which have a great ability to attract the electrons and strengthen the spin coupling, so an excessive coupling is rational to exist in this structure. While in the noA case, two nitroxide groups are link to two conjugated bonds that respectively belong to aromatic imidazole and pyrimidine ring, which is relatively weak to accept the electrons from the outside since they are electronic stable Kekule structures. But it is noticed that in the site 5, the O atom of that nitroxide group has a

hydrogen-bond interaction with the amino group of pyrimidine ring, which makes it more willing to be negative and attract the electrons from outside such as N atom of nitroxide, thus in two resonant structures of nitroxide group ( $>\text{N}^{\cdot-}\text{O}^{\cdot} \leftrightarrow >\text{N}^{\delta+}\text{O}^{\delta-}$ ), the latter is favorable to be formed, resulting in a greater spin delocalization and strong coupling, so the excessive coupling in the noA case is also understandable. The DM noT and noA further verify the strong influence of the bond type of the coupling path and the chemical environment around the nitroxide group in tuning the spin coupling mode of para-position N,N-dioxide system, respectively.

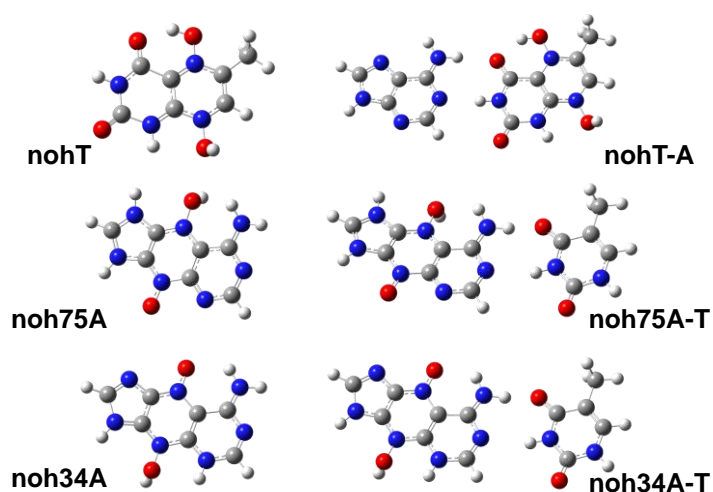


**Fig. S2** The optimized geometries of six nonplanar structures at the HF/6-311++g(d,p) level.

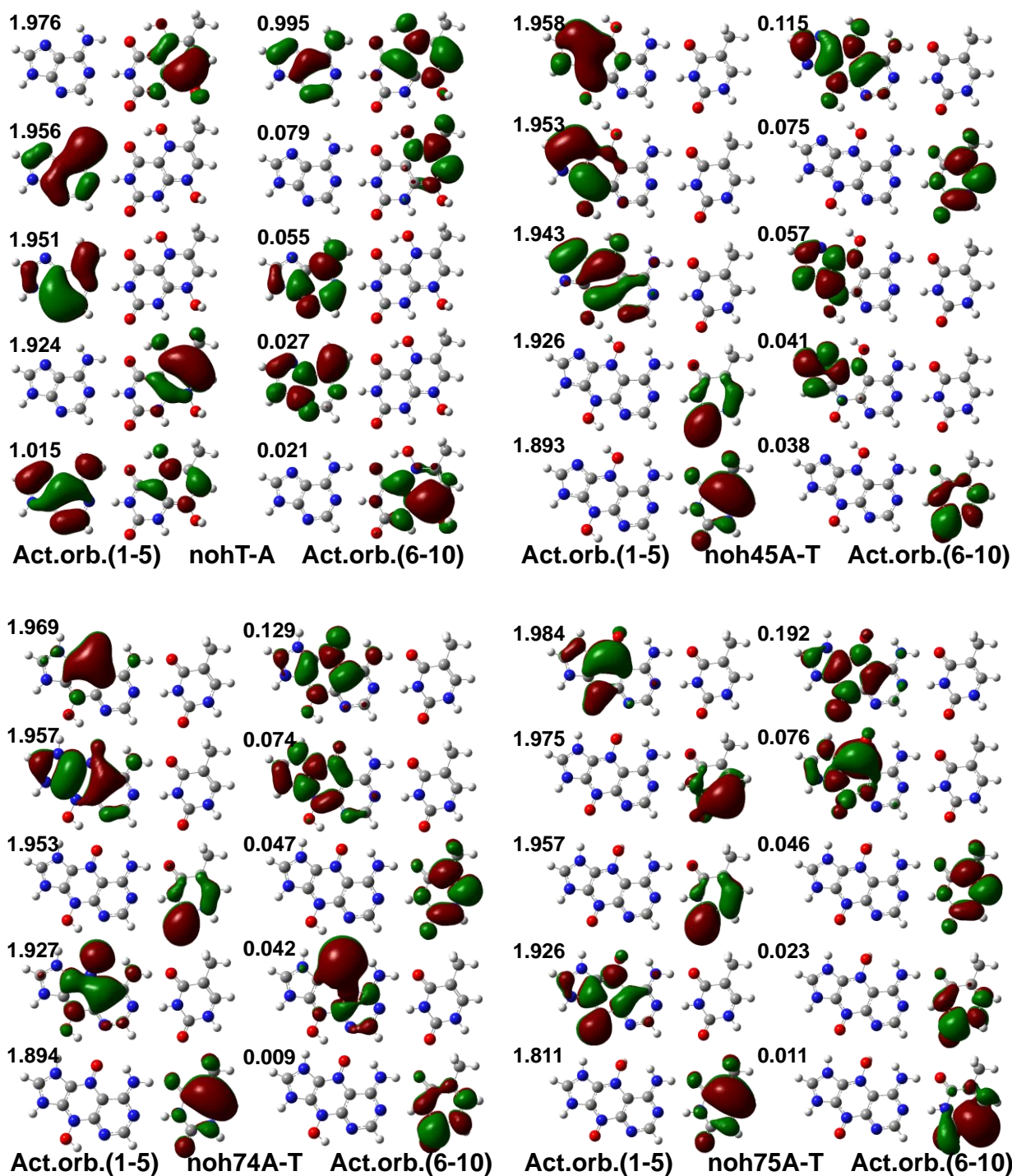


**Fig. S3** The CASSCF-calculated maps and occupation numbers of all the ten active orbitals (Act. orb. 1-10) of four AFM topic base pairs.

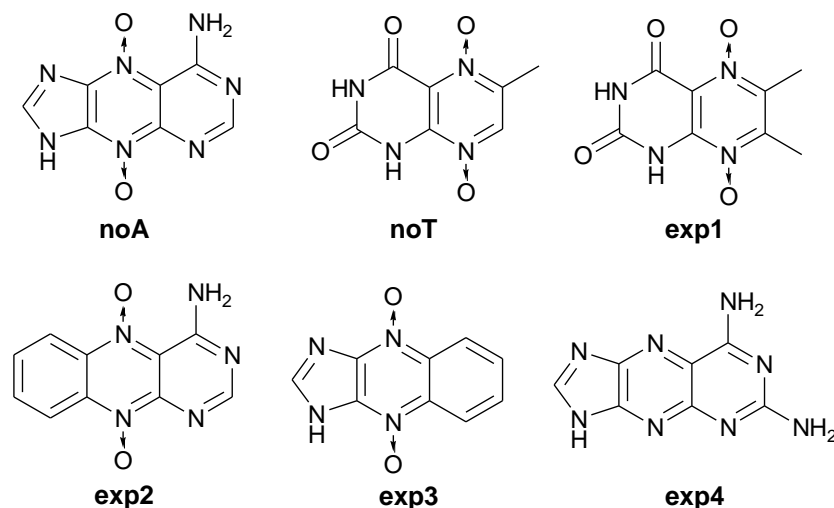


**Fig. S4** The molecular structural formulas of noA, noT and four similar experimentally reported structures respectively named **exp1** (W. Pfeleiderer and W. Hutzenlaub, 1973, **106**, 3149-3174), **exp2** (M. Waly, S. Elgogary, A. Lashien and A. Farag, *J. Heterocyclic Chem.*, 2015, **52**, 411-417), **exp3** (A. S. Elina, I. S. Musatova and L. G. Tsyurul'nikova, *Chem. Heterocycl. Comp.*, 1972, **8**, 1144-1148) and **exp4** (E. C. Taylor and W. R. Sherman, *J. Am. Chem. Soc.*, 1959, **81**, 2464-2471).

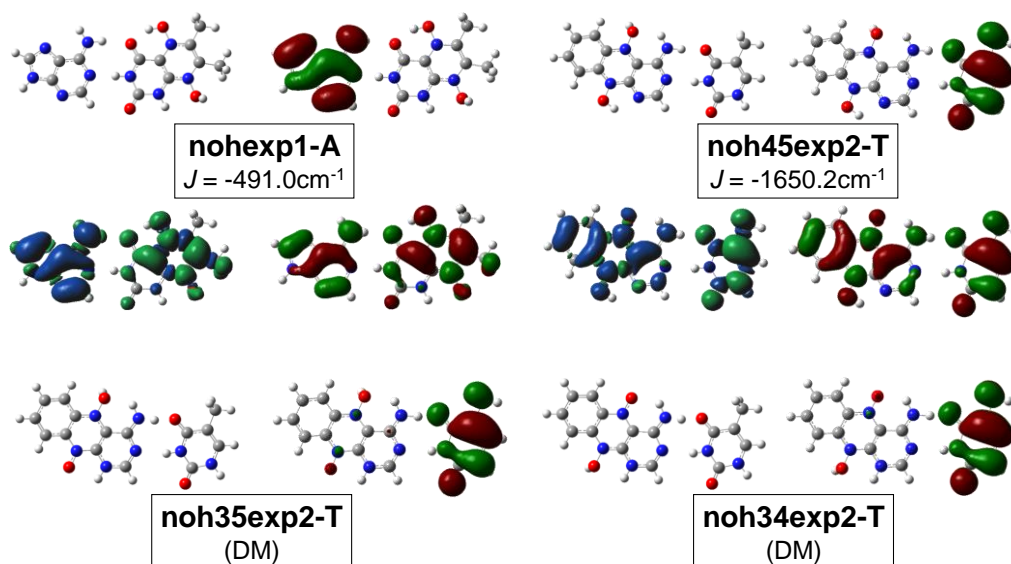


**Fig. S5** The optimized geometries, calculated magnetic properties, SOMOs and spin density maps of AFM base pairs or HOMO maps of DM base pairs for four modified base pairs when using exp1 and exp2 to replace noT and noA for magnetic modification.

**The exploration of magnetic modification of exp1 and exp2.** To further explore the experimentally fundamentals of our designed magnetic modified base pairs, we have found four experimentally reported structures that are very similar with the beginning structures of our two-step modification, noA and noT, as shown in Fig. S4. Then we replace noT by **exp1**, the only difference of which is just one more methyl, and replace noA by **exp2**, in which the imidazole is substituted by benzene. Since the number of protonation sites in **exp2** is half less than noA, only four modified base pairs are needed to be considered, and the calculated results as well as molecular orbitals and spin density maps are placed in Fig. S5. It can be seen that no**exp1**-A has more AFM characters than nohT-A, as reflected in the bigger  $|J|$  value of the former compared with the latter ( $-194.6 \text{ cm}^{-1}$ ), while the  $|J|$  value of noh45**exp2**-T are decreased compared with noh45A-T ( $-2147.2 \text{ cm}^{-1}$ ). In addition, when protonation occurs on site “3”, as noh35**exp2**-T and noh34**exp2**-T show, DM characters are also obtained, which further confirms the fact that “3” protonation site is unfavorable for the electron separation effect and the generation of diradical character.

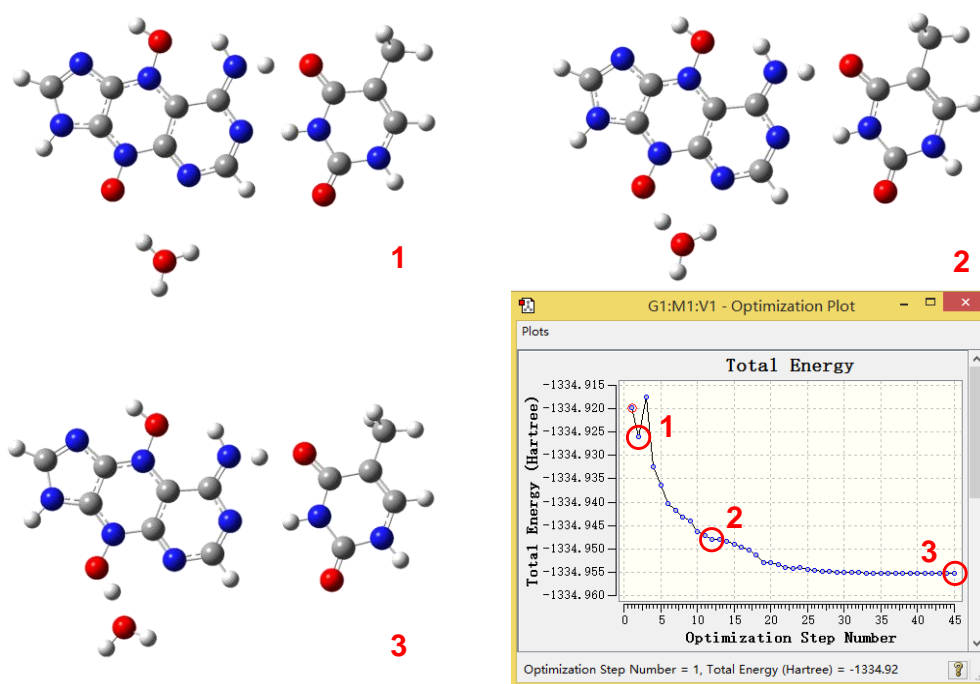


**Fig. S6** The energy curve and some intermediate geometries of the optimization process of noh5A-T...(4-site)  $\text{H}_3\text{O}^+$  structure.

**Simple analysis for the continuously declined energy curve in Fig. S6.** The six single protonation base pairs are respectively named as noh3A-T, noh4A-T, noh5A-T, noh7A-T, noh1T-A, noh2T-A, and the protonation site “1” or “2” in nohT-A mean the protonation site which is close to or far from the methyl group of noT. As shown in Fig. S6, we want to get the optimized geometry of noh5A-T⋯(4-site) H<sub>3</sub>O<sup>+</sup> (structure “1”), but we finally get the structure of noh45A-T⋯H<sub>2</sub>O (structure “3”) with a continuously falling energy curve, meaning that the proton transfer from H<sub>3</sub>O<sup>+</sup> to noh5A-T may be spontaneous/exothermic. This may be due to the special reaction path of the proton transfer process. Structure “2” of Fig. S6 shows a stable configuration of noh5A-T⋯(4-site) H<sub>3</sub>O<sup>+</sup>, in which two H-bonds are generated. We calculate the protonation and diprotonation energies of all considered bases (Table S6). All results indicate that the double protonations are favorable for the present cases, and are easily realized although two protons are repulsive in the protonation processes.

Other structures have the same situation with the example in Fig. S6.

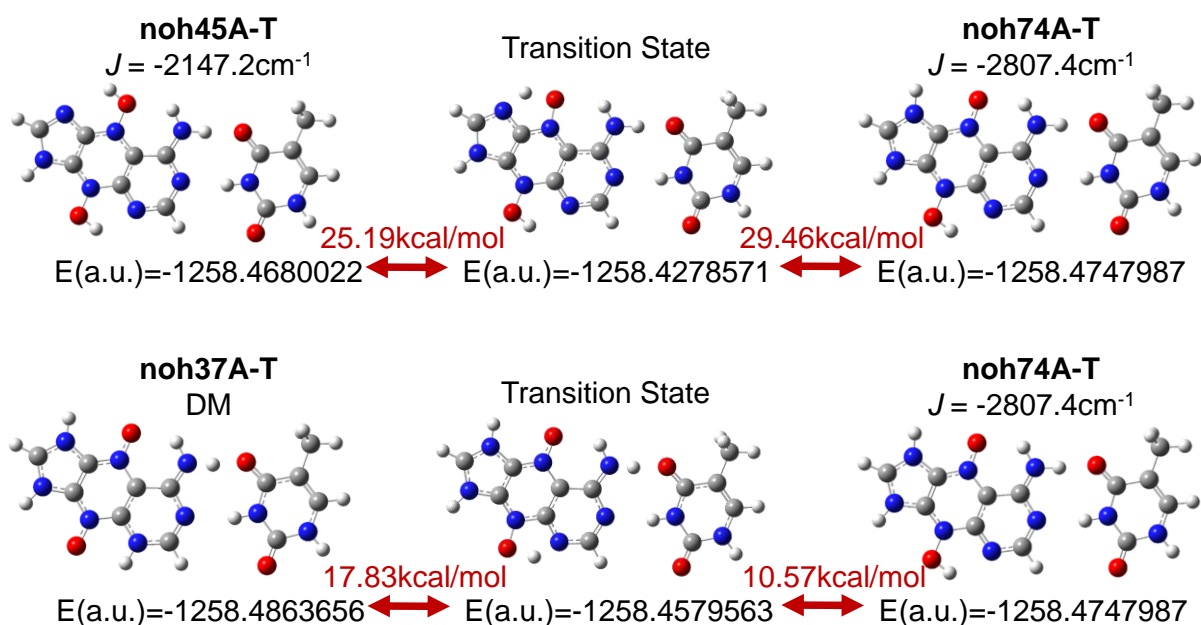


**Fig. S7** Optimized transition state and calculated activation energy of prototropic tautomerization among noh45A-T, noh74A-T, and noh37A-T.